

We are IntechOpen, the world's leading publisher of Open Access books Built by scientists, for scientists

6,900

Open access books available

186,000

International authors and editors

200M

Downloads

Our authors are among the

154

Countries delivered to

TOP 1%

most cited scientists

12.2%

Contributors from top 500 universities



WEB OF SCIENCE™

Selection of our books indexed in the Book Citation Index
in Web of Science™ Core Collection (BKCI)

Interested in publishing with us?
Contact book.department@intechopen.com

Numbers displayed above are based on latest data collected.
For more information visit www.intechopen.com



Synthesis of WO₃ Nanostructures and Their Nanocomposites with Graphene Derivatives via Novel Chemical Approach

Rhizlane Hatel and Mimouna Baitoul

Abstract

Trioxide Tungsten (WO₃), an n-type semiconductor that exhibits a wide band gap of 2.5 to 3.6 eV, has attracted special attention from the scientific community. This attraction is due to its manifold properties, which not only follow the development of technologies, but accelerate it. There are several methods to synthesize WO₃ nanostructures with various morphologies. In the present study, for the first time, a novel chemical method was developed for the preparation of WO₃ nanostructures by using tungsten carbide (WC) as precursor. This novel approach has many advantages such as high yields, simple methodology and easy work up. Moreover, graphene oxide coated with WO₃ nanostructured is prepared via in-situ and ex-situ chemical approaches followed by subsequent thermal treatment at 500°C. The obtained samples were characterized by different techniques to confirm the transformation of WC to WO₃ nanostructures and the formation of their nanocomposites with graphene derivatives.

Keywords: trioxide tungsten, tungsten carbide, nanocomposites, graphene oxide

1. Introduction

Nanocomposites based on nanocarbons and nanostructured metal oxides (NMO) offer the possibility of improving the performance of several devices and developing multifunctional systems by combining the properties of each individual phase. The importance of choosing an appropriate route for the preparation of these nanocomposites has led scientists to take an interest in the development of synthetic methods that are versatile, generalized and easily adaptable to prepare various nanocomposites [1].

Among various NMO, nano-sized (WO₃) structures are of great interest due to their stability in aqueous solution, good crystal quality, remarkable charge transport and unique optical properties [2]. With these manifold properties, they have already been widely used in photocatalysts, photonics and electronics devices [3]. For most of these applications, many physical and chemical approaches have been developed to synthesize WO₃ nanostructures using common precursors such as Na₂WO₄ and WCl₆ [4]. JAMALI et al. recently have reported sol-gel method and its effect on the structural and morphological properties of WO₃ nanostructures [5].

As well as, Tehrani et al. have prepared 1D and 2 D WO_3 by hydrothermal treatment [6]. However, to the best of our knowledge this is the first study about the synthesis of WO_3 nanostructures using tungsten carbide WC as precursor through chemical oxidation approach.

The combination of these nanostructures with nanocarbons in general and graphene derivatives in particular have attracted considerable interest in the scientific community. Graphene oxide (GO) is a single or few layers of oxidized graphite, just like graphene considered as a single layer of graphite [7]. It has been defined as an important precursor of graphene and the basic material for the development of graphene-based nanocomposites [8]. Furthermore, the synthesis of these kinds of nanocomposites having a well-defined structure represents a problem with the methods requiring particular conditions. The key challenge, to improve their performance and broaden their field of application, is to develop simpler synthetic methods in order to increase the control during the formation and the anchoring of nanostructures on the surface of nanocarbons, while maintaining the structural integrity of the composite at the nanoscale.

To date, nanocomposites with different morphologies can be prepared by various methods that can be classified into two categories: ex situ hybridization and in situ crystallization [9]. Ex-situ hybridization involves mixing the pre-synthesized nanocarbons and NMO [10]. Prior to mixing, surface modification of nanostructures and/or nanocarbons is often required, so that they can bind either through covalent or non-covalent interactions including Van der Waals interactions, hydrogen bonds or electrostatic interactions. In addition, the type of functionalization and the strength of the interaction determine the distribution of metal oxide nanoparticles on the surface of the nanocarbons. Although ex-situ hybridization is able to pre-select nanostructures with desired functionality, it sometimes suffers from the low density and non-uniform distribution of nanostructures on nanocarbon surfaces. However, in-situ crystallization can give rise to uniform surface distribution of nanoparticles by controlling nucleation sites on nanocarbons via surface functionalization. As a result, a continuous film of nanoparticles on surfaces can be achieved [11].

In this work, we developed for the first time, a new and simple method to synthesize the nanostructures of WO_3 and their nanocomposites by in situ and ex situ chemical approaches. The synthesis process is based on simple chemical oxidation and subsequent thermal annealing. Moreover, in order to validate the feasibility of our approaches, we examine our samples obtained by different techniques such as X-ray diffraction (XRD) to analyze structural properties, scanning electron microscopy (SEM) to determine morphology, shape and size of nanostructures, as well as Fourier transform infrared (FTIR) to elucidate the vibrational behavior and the type of interaction between the different constituents.

2. WO_3 nano-sized structures

2.1 Synthesis method

The synthesis of WO_3 nanostructures involved two steps. In the first step, 1 g of WC and 10 ml of H_2SO_4 were mixed and stirred in an ice bath. This mixture was continuously stirred while 3 g of KMnO_4 was added slowly over 1 h, the temperature was kept below 20°C . After adding KMnO_4 , the mixture was stirred for a further 2 h, 15 ml H_2O_2 (30 wt% aqueous solution) was slowly added and then the resulting solution turned into homogenous yellow color and was left to stir for another 2 h. The product was centrifuged and dried in the oven at 60°C . In the

second step, the obtained yellow powder corresponding to tungsten oxide hydrate WO₃.H₂O was dispersed in a mixture of water and ethanol (1, 5), dropped onto a glass substrate and heated in a furnace up to 500°C at the heating rate of 10°C min⁻¹. The sample was kept inside the furnace at the mentioned temperature for 5 h [12].

2.2 Characterization

Structural information of different tungsten-based materials are shown in **Figure 1**. The WC diffraction spectrum shows three major intense peaks located at $2\theta = 31.57^\circ$, 35.72° and 48.40° which correspond well to the crystallographic planes (001, 100, 101) of WC, respectively. The positions of the peaks are in good agreement with the JCPDS reference (N: 65–4539), which confirm the hexagonal structure of WC, of space group P6m2, with the parameters $a = 2.906 \text{ \AA}$ and $c = 2.838 \text{ \AA}$. According to a study carried out on the oxidation of WC to WO₃ via a dry synthetic route in air and at high temperature [13], the authors found that tungsten carbide oxidizes more quickly than tungsten metal. However, the oxidation WC chemical with precise size control has never been reported to our knowledge.

After oxidation, we can identify the crystalline nature of the prepared sample by analyzing its X-ray diffraction (XRD) spectrum. All the diffraction peaks are well indexed to tungsten oxide monohydrate WO₃.H₂O with an orthorhombic phase (JCPDS N: 43–0679, of space group: Pmnb (62) having the lattice parameters: $a = 5.238 \text{ \AA}$, $b = 10.704 \text{ \AA}$ and $c = 5.12 \text{ \AA}$). The peaks are intense and narrow, indicating better crystallinity. Additionally, no peak of impurities and/or other hydrated phase such as WO₃.2H₂O and WO₃.0.33H₂O was observed in the spectrum [14, 15]. Indeed, this material has been widely used as a precursor for the synthesis of the monoclinic and hexagonal phases of WO₃, which are different in their geometry and their stability [16]. The hexagonal phase is metastable, while the monoclinic phase is the most stable than all other structures of WO₃ due to its pseudo-cubic structure made up of a three-dimensional array of WO₆ octahedra [17].

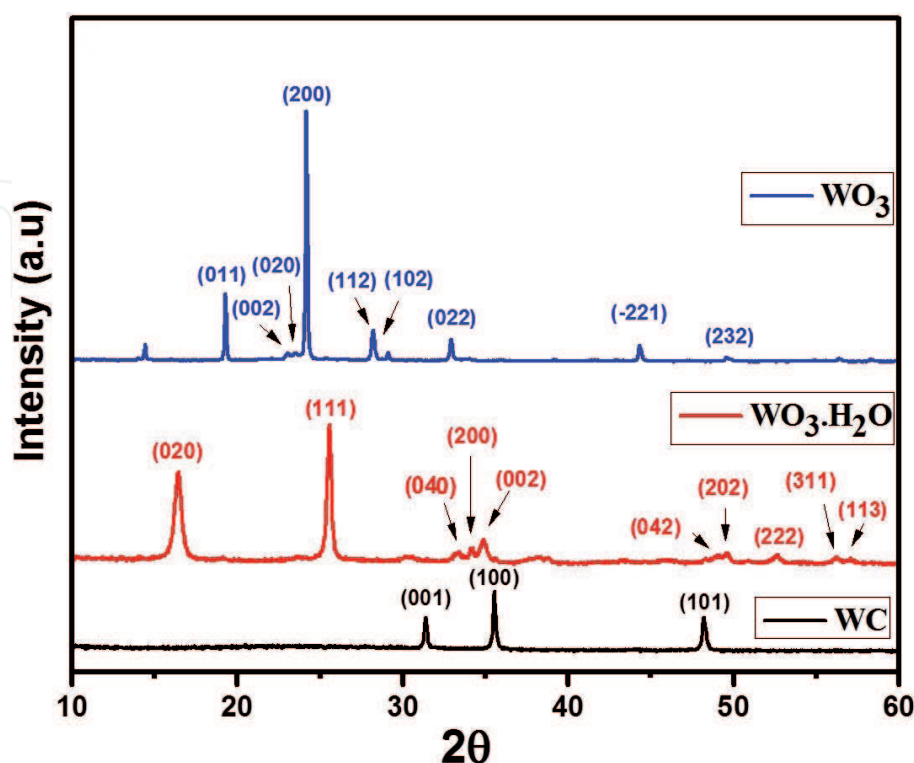


Figure 1.
 X-ray diffraction patterns of WC, WO₃.H₂O, WO₃ nanostructures.

During the heat treatment at 500°C, $\text{WO}_3 \cdot \text{H}_2\text{O}$ as synthesized gradually dehydrates until it turns completely into WO_3 . **Figure 1** blue spectrum shows a series of diffraction peaks at $2\theta = 19.26^\circ, 23.07^\circ, 23.45^\circ, 24.17^\circ, 28.22^\circ, 29.13^\circ, 32.86^\circ, 44.3^\circ$ and 49.6° which correspond to the crystallographic planes (011, 002, 020, 200, 112, 102, 022, 320, 232). The positions of these peaks are consistent with those expected for the WO_3 monoclinic phase reported in the JCPDS N: 43–1035 file, of space group: P21/n (14) and lattice parameters: $a = 7.297 \text{ \AA}$, $b = 7.539 \text{ \AA}$ and $c = 7.688 \text{ \AA}$.

The crystallite size was calculated, using the Scherrer equation, for all tungsten-based components, as shown in **Table 1**. The results obtained demonstrate the growth in the size of the crystallites of WO_3 as a function of the annealing temperature. Gui et al. synthesized WO_3 with monoclinic phase using the hydrothermal route and WCl_6 as a precursor, they estimated a particle size of the order of 22 nm [18]. Fu et al. reported a value, similar to our result, of around 42 nm hydrothermally treated at 180°C for 24 h, using $\text{Na}_2\text{WO}_4 \cdot 2\text{H}_2\text{O}$ as a precursor [19].

Material	Plan	2θ	Intensity	Size (nm)	Average size (nm)
WC	(001)	31.4°	0.56	39.32	36
	(100)	35.4°	0.98	39.28	
	(101)	48.2°	0.57	28.4	
$\text{WO}_3 \cdot \text{H}_2\text{O}$	(020)	16.4°	0.66	17.28	21
	(111)	25.4°	0.98	31.78	
	(040)	33.2°	0.11	18.07	
	(200)	34.1°	0.14	36.18	
	(002)	34.9°	0.19	17.65	
WO_3 (500°C)	(011)	13.31°	0.27	50.2	57
	(002)	23°	0.042	62	
	(020)	23.4°	0.038	67	
	(200)	24.1°	0.98	56.18	
	(112)	28.19°	0.12	50.65	

Table 1.
Crystallites size of tungsten-based nanomaterials.

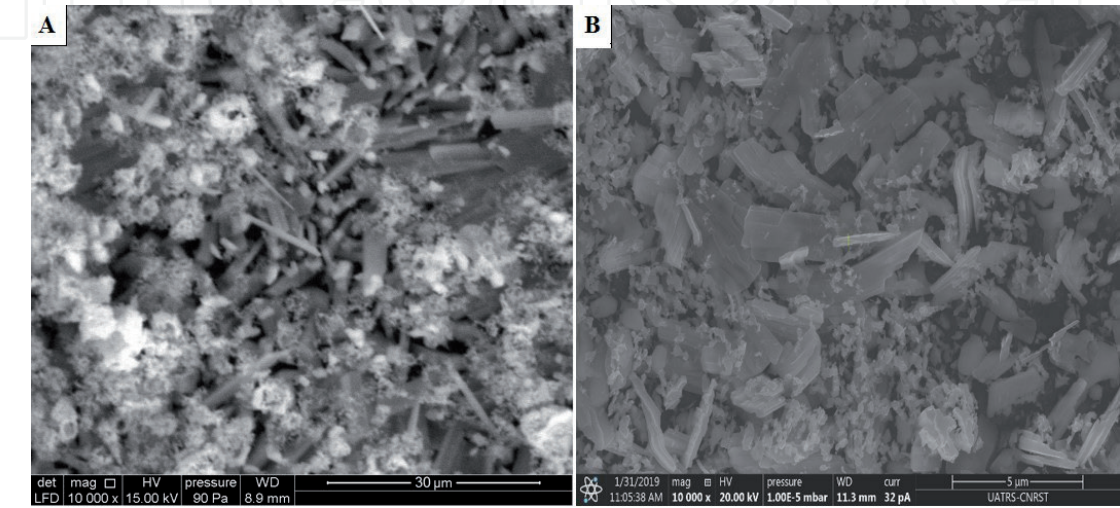


Figure 2.
SEM images of WO_3 nanostructures.

The morphology observation is performed to investigate the surface and the shape of the nanostructured WO₃. As seen from the SEM image (**Figure 2A**). The morphology obtained after a heat treatment at 500°C is effectively homogeneous and composed of what are called nanorods, with the presence of a few hollow nanospheres. In **Figure 2B**, WO₃ nanorods are clearly observed. Choi et al. demonstrated different morphologies of WO₃ such as nanowires, nanorods and nanosheets by varying the volume of water (%) and ethanol [20]. Marques et al. have prepared different morphologies including nanoplates and nanoflowers by varying the initial precursor and the pH of the medium [21].

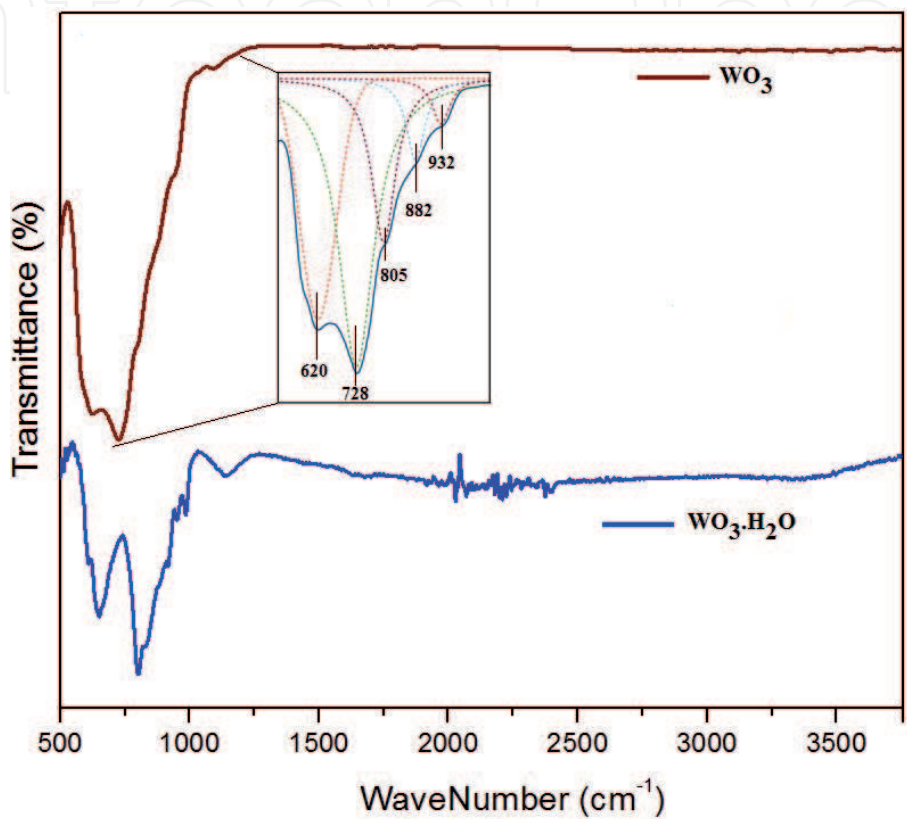


Figure 3.
FT-IR spectra of WO₃.H₂O, WO₃ nanostructures.

Material	Frequency (cm ⁻¹)	Attribution
WO ₃ .H ₂ O	602	γ (W-O-W)
	650	δ (O-W-O)
	883	ν (W-O-W)
	985	ν (W=O)
	1139	ν (W-OH)
	3440	ν (-OH)
WO ₃ (500 °C)	620	γ (W-O-W)
	728	δ (O-W-O)
	805	ν (O-W-O)
	882	ν (W-O-W)
	932	ν (W=O)

Table 2.
Tungsten oxide infrared bands and their attributions.

In order to determine the exact composition of the sample, and to gain more information on its crystal structure, FTIR measurement was implemented.

In the range between 500 and 1000 cm^{-1} (**Figure 3**), multi-bands are observed, attributed to tungsten-oxygen elongation vibrations including elongation vibrations (ν), in-plane bending vibrations (δ) and out of plane (γ), as shown in **Table 2**. These characteristic bands prove the successful synthesis of WO_3 monoclinic phase.

3. GO/ WO_3 nanocomposites

3.1 GO/ WO_3 prepared in-situ

3.1.1 Synthesis method

For the in situ method, the nanocomposite was prepared using the same process as that used for WO_3 ; but with the presence of graphite powder. As shown in **Figure 4**, after the interaction of WC with KMnO_4 and H_2SO_4 solution for 1 h in an ice bath, a small amount of graphite powder was added and the mixture kept under mechanic agitation for 2 h. Then, H_2O_2 was added and the resulting solution turned into green-brown color. The homogeneous solutions obtained were slowly dropped onto glass substrate, and heated at 500°C for 5 h.

3.1.2 Characterization

The obtained XRD patterns are shown in **Figure 5**. In the case of the nanocomposite prepared in situ from graphite and WC, we note that the position and intensity of the peaks obtained have been greatly modified. The main peaks of the monoclinic phase are reduced in intensity and several peaks have appeared corresponding to other polymorphs of WO_3 , including the hexagonal, orthorhombic phases and substoichiometric chemical compositions [22, 23].

The appearance of a similar multi-phase structure is consistent with the fact that the in situ insertion of graphite leads to the modification of the crystal structure formed of tungsten oxide. Some of the more well-known non-stoichiometric compositions of WO_x are $\text{W}_{17}\text{O}_{48}$, $\text{W}_{20}\text{O}_{58}$, $\text{W}_{18}\text{O}_{49}$ and $\text{W}_{24}\text{O}_{68}$. Such oxides are formed by the sharing of vertices of WO_6 octahedra, which alternate with those which are partially established by sharing the edges [24].

Oxygen removal occurs through the crystal shear mechanism and as the x value in WO_x decreases, the WO_6 octahedra groups form closer shear planes. However, for x values close to 3, these planes are considered as extended defects. On the other hand, with a further decrease in x , the shear planes tend to interact with each other and align in parallel, filling the space between them with sharing vertices of WO_6 octahedra. For x less than or equal to 2.87, the structure becomes unstable

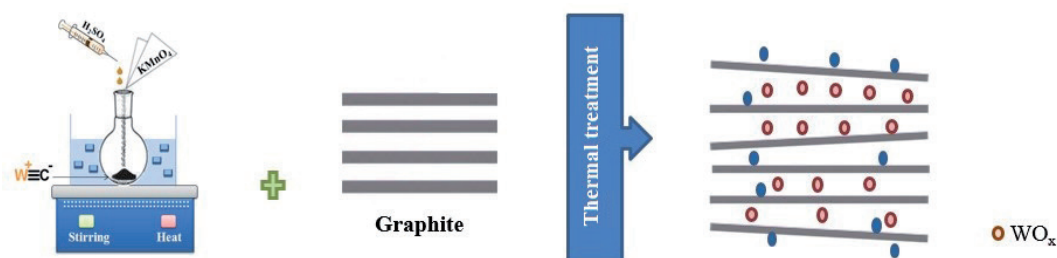


Figure 4.
Preparation method of in-situ nanocomposite.

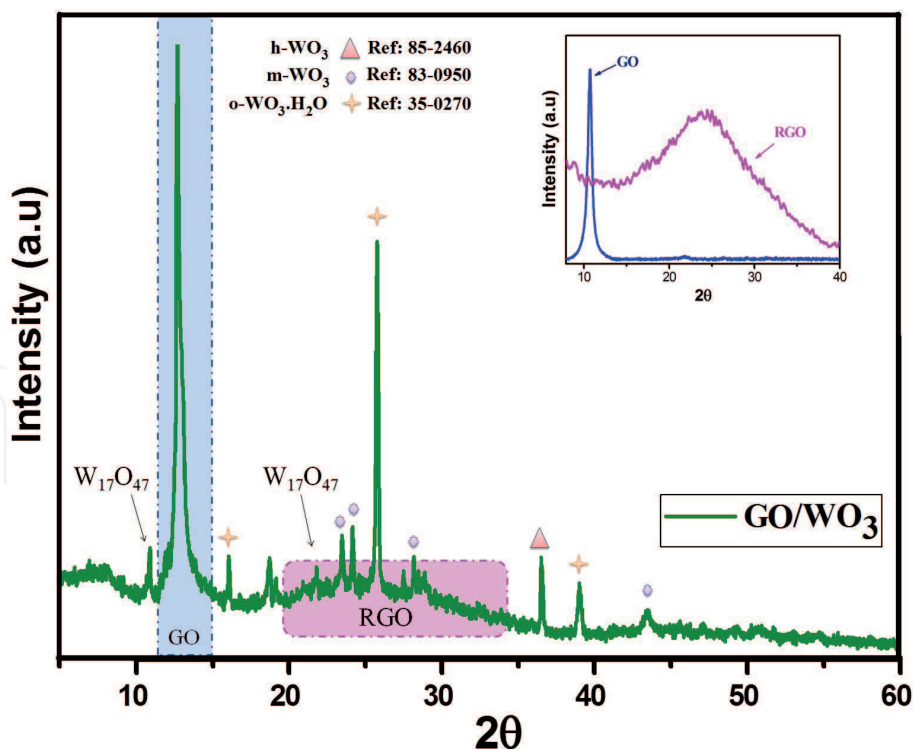


Figure 5.
 X-ray diffraction of GO/WO₃ in-situ prepared nanocomposite.

and further restructuring occurs involving the formation of pentagonal columns parallel to the monoclinic axis that are either single or paired by partitioning of the edges. Moreover, recent studies [25] have shown that non-stoichiometric tungsten oxide nanostructures have better performance in advanced applications. They have shown that the oxygen deficiencies presented in these nanomaterials can be major assets for storing energy. In addition, the X-ray diffraction pattern of the nanocomposite shows an intense peak characteristic of graphene oxide located at $2\theta = 12.73^\circ$ and assigned to the (002) plane with an interlayer “d” spacing of 6.95 Å, which is quite high compared to graphite (3.36 Å) and slightly lower than that of GO (7.93 Å) obtained by the Hummer method and in the absence of WC. The appearance of a small and wide band around $23\text{--}26^\circ$ confirms the formation of a few partially oxidized graphite nanosheets.

Indeed, the modification of the spacing between the layers of graphite is directly correlated to their exfoliation through the introduction of the metal oxide nanostructures formed which also causes the modification of the Van der Waals interaction. In addition, it should be noted that the appearance of a multiphase structure could be due to the fact that the in-situ insertion of graphite has a strong influence on the orientation and length of the tungsten-oxygen bond, resulting in non-stoichiometric WO_x nanostructures.

SEM image is used to investigate the microscopic structure of the obtained sample. **Figure 6** shows the morphological aspect of in situ GO/WO₃ nanocomposite. The presence of graphene layers functionalized by spherical-shaped WO₃ nanostructures distributed randomly can be detected. This nanocomposite has a stable structure reducing the agglomeration of graphitic planes and indicating the interfacial interaction between the two components. These results are in good agreement with those obtained by X-ray diffraction.

The infrared spectrum of nanocomposite prepared in situ (**Figure 7**) exhibits a broad absorption band at 640 cm^{-1} attributed to the W-O-W vibration, and another band at 982 cm^{-1} characteristic of the short elongation bond W = O [26]. This is explained by the fact that the in situ preparation of tungsten oxide nanostructures

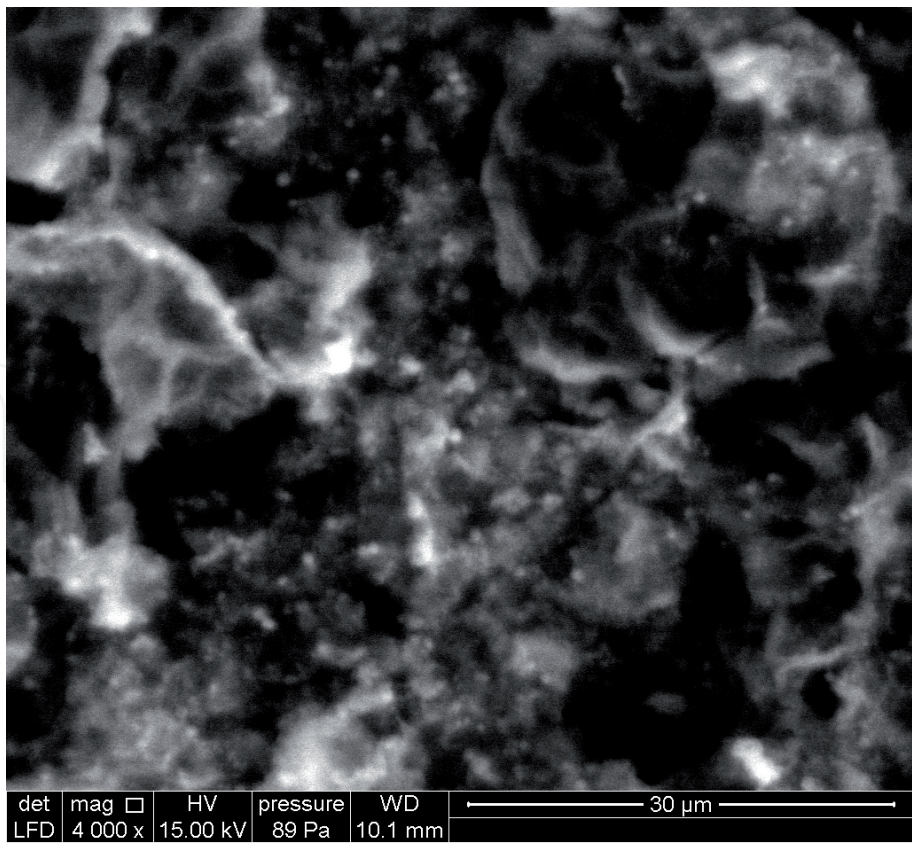


Figure 6.
SEM image of GO/WO₃ in-situ prepared nanocomposite.

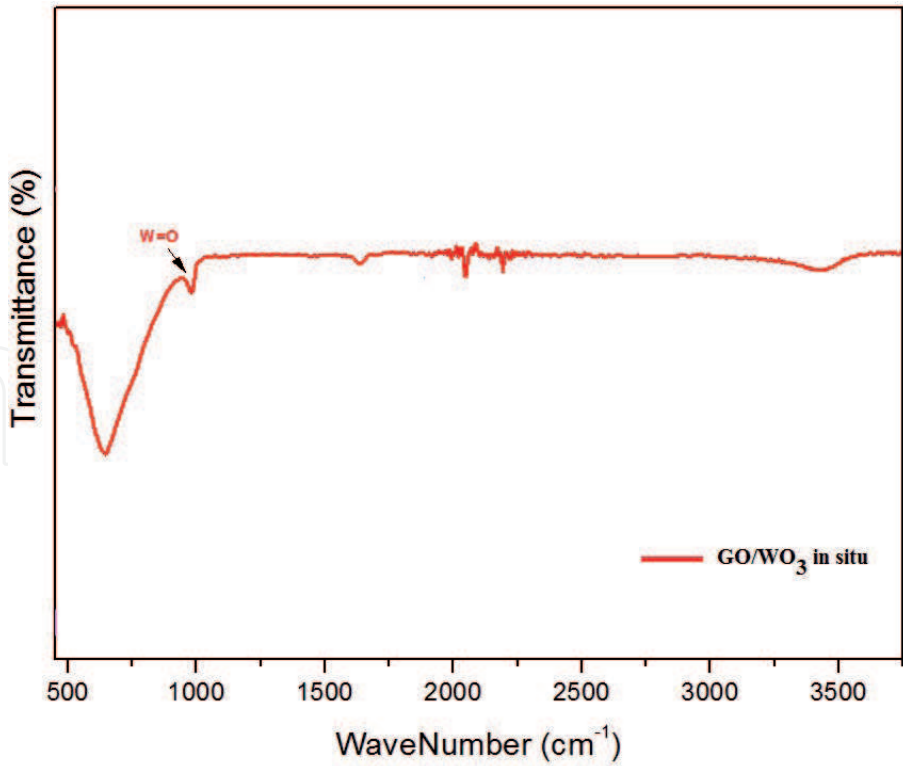


Figure 7.
FT-IR spectrum of GO/WO₃ in-situ prepared nanocomposite.

in the presence of graphite leads to the formation of non-stoichiometric WO_x nanostructures. In fact, during the interaction, the vibration modes linked to the single WO bonds gradually weakened, while the W = O double bonds are formed by

increasing the areas of the boundaries and creating more deficit in atoms of oxygen, which contributes to the modification of the crystallographic structure. These results are in good agreement with those obtained by XRD.

3.2 GO/WO₃ prepared ex-situ

3.2.1 Synthesis method

GO/WO₃ nanocomposite was synthesized by mixing solutions of hydrated tungsten oxide and graphene oxide. In a typical procedure, the solution of WO₃.H₂O was mixed with that of GO, then the resulting mixture is placed in an ultra-sonic bath for 30 min at room temperature. After deposition on the glass substrate and calcination at 500°C., the GO/WO₃ nanocomposite was obtained with a mass ratio of 1: 1 (**Figure 8**).

3.2.2 Characterization

The XRD spectrum in **Figure 9** reveals the crystal structure of the GO/WO₃ nanocomposites prepared ex situ and treated at 500°C. The diffractogram of the nanocomposite is dominated by the peaks characteristic of the monoclinic phase of WO₃ [JCPDS N: 26–0575]. The three main peaks at $2\theta = 23.07^\circ$, 23.45° , 24.17° characteristic of this phase are overlapped with the broad band corresponding to reduced GO.

The same behavior was obtained for the RGO/WO₃ nanocomposite prepared by the hydrothermal method, as well as GO/ZnO and GO/TiO₂ nanocomposites prepared ex situ [22–24]. It is well known that the formation of reduced GO is confirmed by the disappearance of the intense peak in GO at 10.9° and the appearance of a larger one around 26° . Due to the oxygenated functional groups on the surface of the carbon planes, aromatic regions with sp^3 networks provide active sites for interacting with other chemical species through interactions at interfaces. Thus, GO is a very important precursor for the preparation of graphene-based composite materials with metals, metal oxides, polymers and CNTs for various applications. Consequently, this result obtained confirms the reduction of GO after the functionalization with WO₃ and the formation of the nanocomposite. Furthermore, no secondary phase was detected, suggesting that the nanostructured WO₃ retained its monoclinic phase after its interaction with the GO nanosheets.

For the morphology of the GO/WO₃ nanocomposite prepared ex situ (**Figure 10**), we observe the presence of the one-dimensional shape with a homogeneous and uniform distribution. The nanorods formed in the presence of GO have lengths lower than those of the WO₃ nanorods alone. In addition, the trace of the GO sheets is not clearly observed, confirming that the GO sheets are covered by the nanostructures of WO₃.

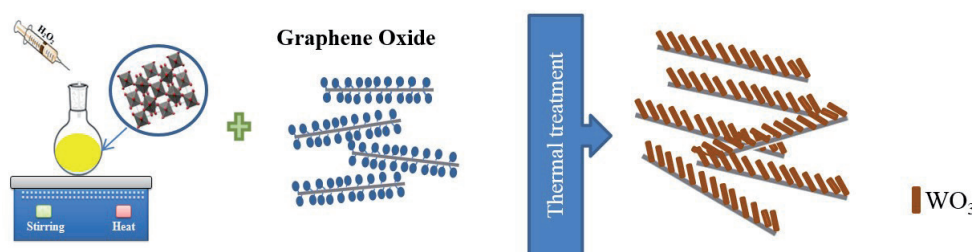


Figure 8.
 Preparation method of ex-situ nanocomposite.

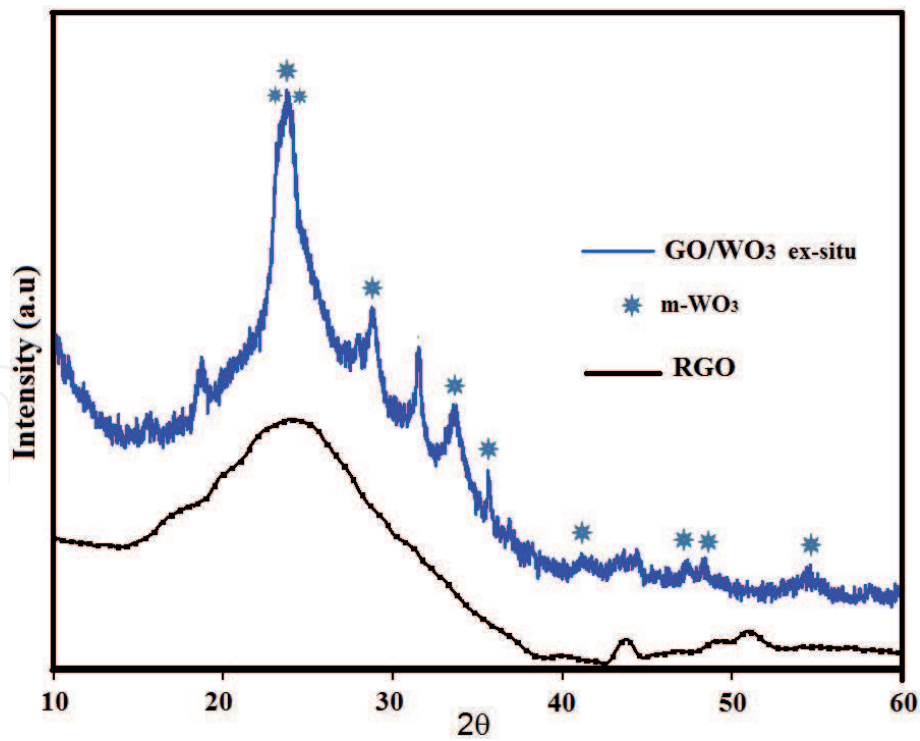


Figure 9.
X-ray diffraction of GO/WO₃ ex-situ prepared nanocomposite.

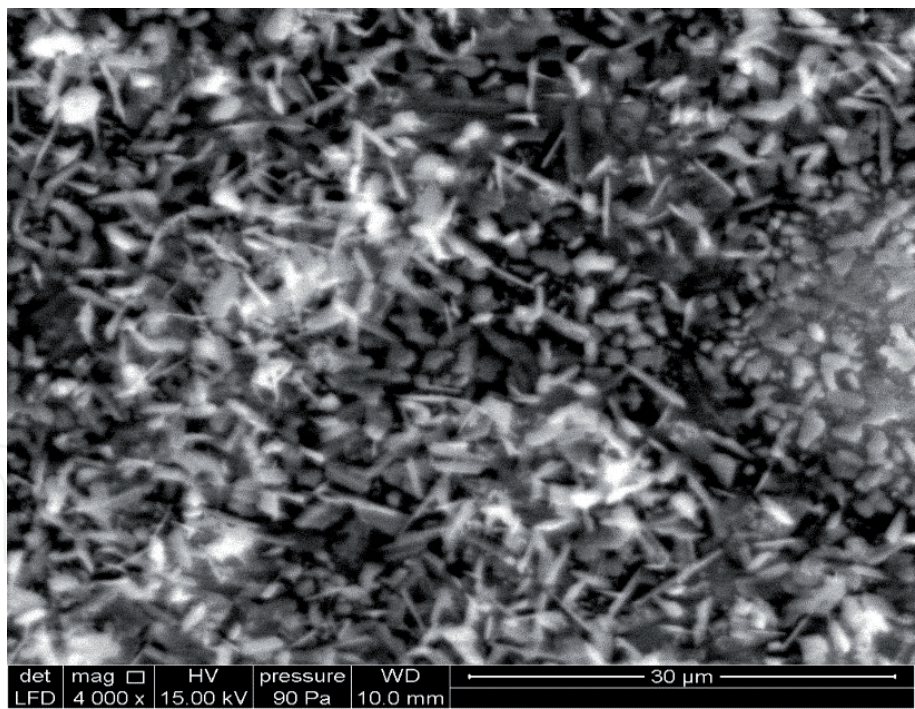


Figure 10.
SEM image of GO/WO₃ ex-situ prepared nanocomposite.

In order to determine the exact composition of the samples as well as the types of interactions between the constituents, the Fourier Transform IR Spectroscopy (FTIR) analysis was performed. In the low-frequency region (**Figure 11**), the nanocomposite prepared ex-situ exhibits the characteristic bands of the W-O bond. In addition, a new band appears at around 1120 cm⁻¹ attributed to the W-O-C link [26]. This result demonstrates that WO₃ nanorods uniformly attach to the GO surface through covalent functionalization.

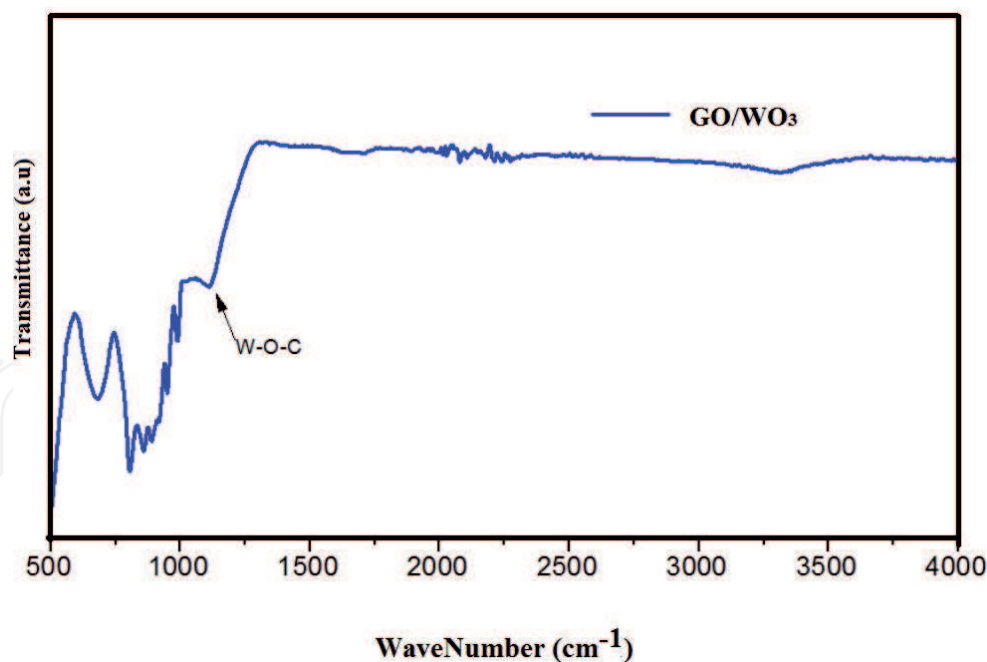


Figure 11.
 FT-IR spectra of GO/WO_3 ex-situ prepared nanocomposite.

4. Conclusion

In summary, we carried out a study of structural, morphological and vibrational properties of tungsten oxide nanostructures and their nanocomposite with GO nanosheets. First of all, we succeeded in synthesizing WO_3 through a new methodology based on the oxidation of WC, using strong acids and oxidizing agents, which allowed us to obtain the hydrated tungsten oxide $\text{WO}_3 \cdot \text{H}_2\text{O}$ as an intermediate product, before being completely transformed by heat treatment at high temperature in air into WO_3 . By using XRD, we were able to identify the different structures, as well as the variation in size of tungsten-based crystallites. In the case of the prepared nanocomposites, we found that graphite and GO have a significant effect on the crystallographic structure, morphology and stoichiometry of the nanostructured tungsten oxide. As result, the in situ prepared WO_3 nanostructures have shown a drastic change in the morphology and the stoichiometry when their growth is initiated in the presence of graphite powder. However, the ex situ preparation of the composite leads to the formation of well-dispersed WO_3 nanorods, with monoclinic phase, covalently bonded to the RGO nanosheets. This study provides a possibility for preparing tungsten oxide nanostructures based nanocomposites with low-cost and no special equipment.

IntechOpen

IntechOpen


Author details

Rhizlane Hatel* and Mimouna Baitoul

Group of Polymers and Nanomaterials, Laboratory of Solid State Physics, Faculty of Sciences Dhar el Mahraz, University Sidi Mohammed Ben Abdellah, Atlas, Fez, Morocco

*Address all correspondence to: hatel.rhizlane@gmail.com

IntechOpen

© 2021 The Author(s). Licensee IntechOpen. This chapter is distributed under the terms of the Creative Commons Attribution License (<http://creativecommons.org/licenses/by/3.0>), which permits unrestricted use, distribution, and reproduction in any medium, provided the original work is properly cited. 

References

- [1] T. Guo, M.-S. Yao, Y.-H. Lin, C.-W. Nan, A comprehensive review on synthesis methods for transition-metal oxide nanostructures, *Cryst. Eng. Comm.* 17 (2015) 3551-3585.
- [2] M. Kumar, Metal oxide nanostructures: growth and applications, *Adv. Nanomater.* 79 (2016) 203-230.
- [3] W. Zhao, B. Cui, H. Qiu, P. Chen, Y. Wang, Multifunctional Fe₃O₄@ WO₃@ mSiO₂-APTES nanocarrier for targeted drug delivery and controllable release with microwave irradiation triggered by WO₃, *Mater. Lett.* 169 (2016) 185-188.
- [4] R. Lei, H. Ni, R. Chen, B. Zhang, W. Zhan, Y. Li, Hydrothermal synthesis of WO₃/Fe₂O₃ nanosheet arrays on iron foil for photocatalytic degradation of methylene blue, *J. Mater. Sci. Mater. Electron.* 28 (2017) 10481-10487.
- [5] W. Wu, Q. Yu, J. Lian, J. Bao, Z. Liu, S.-S. Pei, Tetragonal tungsten oxide nanobelts synthesized by chemical vapor deposition, *J. Cryst. Growth* 312 (2010) 3147-3150.
- [6] S. Bai, K. Zhang, L. Wang, J. Sun, R. Luo, D. Li, A. Chen, Synthesis mechanism and gas-sensing application of nanosheet-assembled tungsten oxide microspheres, *J. Mater. Chem. A* 2 (2014) 7927-7934.
- [7] Y.M. Shirke, S.P. Mukherjee, Selective synthesis of WO₃ and W₁₈O₄₉ nanostructures: ligand-free pH-dependent morphology-controlled self-assembly of hierarchical architectures from 1D nanostructure and sunlight-driven photocatalytic degradation, *Cryst. Eng. Comm.* 19 (2017) 2096-2105.
- [8] A.S. Kurlov, A.I. Gusev, Oxidation of tungsten carbide powders in air, *Int. J. Refract. Metals Hard Mater.* 41 (2013) 300-307.
- [9] L. Wang, Z. Wei, M. Mao, H. Wang, Y. Li, J. Ma, Metal oxide/graphene composite anode materials for sodium-ion batteries, *Energy Stor. Mater.* 16 (2019) 434-454.
- [10] S.G. Chatterjee, S. Chatterjee, A.K. Ray, A.K. Chakraborty, Graphene-metal oxide nanohybrids for toxic gas sensor: a review, *Sensor. Actuator. B Chem.* 221 (2015) 1170-1181.
- [11] R. Hatel, M. Goumri, B. Ratier, M. Baitoul, Graphene derivatives/Fe₃O₄/polymer nanocomposite films: optical and electrical properties, *Mater. Chem. Phys.* 193 (2017) 156-163.
- [12] J. Kaur, K. Anand, K. Anand, R.C. Singh, WO₃ nanolamellae/reduced graphene oxide nanocomposites for highly sensitive and selective acetone sensing, *J. Mater. Sci.* 53 (2018) 12894-12907.
- [13] M. Khenfouch, U. Buttner, M. Baitoul, M. Maaza, Synthesis and characterization of mass produced high quality few layered graphene sheets via a chemical method, *Graphene* 3 (2) (2014) 7-13.
- [14] M. Ahmadi, M.J.-F. Guinel, Synthesis and characterization of tungstite (WO₃·H₂O) nanoleaves and nanoribbons, *Acta Mater.* 69 (2014) 203-209.
- [15] D. Sandil, S. Srivastava, B.D. Malhotra, S.C. Sharma, N.K. Puri, Biofunctionalized tungsten trioxide-reduced graphene oxide nanocomposites for sensitive electrochemical immunosensing of cardiac biomarker, *J. Alloy. Comp.* 763 (2018) 102-110.
- [16] M.A. Fraga, A. Contin, L.A.A. Rodríguez, J. Vieira, R.A. Campos, E.J. Corat, V.J.T. Airolidi, Nano-and microcrystalline diamond deposition on pretreated WC-Co substrates:

structural properties and adhesion, *Mater. Res. Express* 3 (2016) 25601.

[17] V. Hariharan, S. Radhakrishnan, M. Parthibavarman, R. Dhilipkumar, C. Sekar, Synthesis of polyethylene glycol (PEG) assisted tungsten oxide (WO₃) nanoparticles for L-dopa bio-sensing applications, *Talanta* 85 (2011) 2166-2174.

[18] L. Ghasemi, H. Jafari, Morphological characterization of tungsten trioxide nanopowders synthesized by sol-gel modified pechini's method, *Mater. Res.* 20 (2017) 1713-1721.

[19] V. Hariharan, V. Aroulmoji, K. Prabakaran, B. Gnanavel, M. Parthibavarman, R. Sathyapriya, M. Kanagaraj, Magnetic and electrochemical behaviour of cobalt doped tungsten oxide (WO₃) nanomaterials by microwave irradiation method, *J. Alloy. Comp.* 689 (2016) 41-47.

[20] J. Jayachandiran, A. Raja, M. Arivanandhan, R. Jayavel, D. Nedumaran, A facile synthesis of hybrid nanocomposites of reduced graphene oxide/ZnO and its surface modification characteristics for ozone sensing, *J. Mater. Sci. Mater. Electron.* 29 (2018) 3074-3086.

[21] M. Shanmugam, A. Alsalmeh, A. Alghamdi, R. Jayavel, In-situ microwave synthesis of graphene-TiO₂ nanocomposites with enhanced photocatalytic properties for the degradation of organic pollutants, *J. Photochem. Photobiol. B Biol.* 163 (2016) 216-223.

[22] C. Chacón, M. Rodríguez-Pérez, G. Oskam, G. Rodríguez-Gattorno, Synthesis and characterization of WO₃ polymorphs: monoclinic, orthorhombic and hexagonal structures, *J. Mater. Sci. Mater. Electron.* 26 (2015) 5526-5531.

[23] W.-H. Hu, G.-Q. Han, B. Dong, C.-G. Liu, Facile synthesis of highly dispersed WO₃·H₂O and WO₃ nanoplates for electrocatalytic hydrogen evolution, *J. Nanomater.* 16 (2015) 23.

[24] A.C. Marques, L. Santos, M.N. Costa, J.M. Dantas, P. Duarte, A. Gonçalves, R. Martins, C.A. Salgueiro, E. Fortunato, Office paper platform for bioelectrochromic detection of electrochemically active bacteria using tungsten trioxide nanoplates, *Sci. Rep.* 5 (2015) 9910.

[25] H. Kalhori, M. Ranjbar, H. Salamati, J.M.D. Coey, Flower-like nanostructures of WO₃: fabrication and characterization of their in-liquid gasochromic effect, *Sensor. Actuator. B Chem.* 225 (2016) 535-543.

[26] J. Meng, J. Pei, Z. He, S. Wu, Q. Lin, X. Wei, J. Li, Z. Zhang, Facile synthesis of gC₃N₄ nanosheets loaded with WO₃ nanoparticles with enhanced photocatalytic performance under visible light irradiation, *RSC Adv.* 7 (2017) 24097-24104.